Identification of the target self-antigens in reperfusion injury

Ming Zhang,[1,2,7] Elisabeth M. Alicot,[7] Isaac Chiu,[1] Jinan Li,[1] Nicola Verna,[3] Thomas Vorup-Jensen,[1] Benedikt Kessler,[2] Motomu Shimaoka,[1] Rodney Chan,[3] Daniel Friend,[3] Umar Mahmood,[6] Ralph Weissleder,[6] Francis D. Moore,[3,5] and Michael C. Carroll[1,2,4]

[1]CBR Institute for Biomedical Research, Inc., [2]Department of Pathology, [3]Department of Surgery, [4]Department of Pediatrics, and [5]Brigham and Women's Hospital, Harvard Medical School, Boston, MA 02115
[6]Center for Molecular Imaging Research, Massachusetts General Hospital and Harvard Medical School, Charlestown, MA 02129
[7]DecImmune Therapeutics, Boston, MA 02115

Reperfusion injury (RI), a potential life-threatening disorder, represents an acute inflammatory response after periods of ischemia resulting from myocardial infarction, stroke, surgery, or trauma. The recent identification of a monoclonal natural IgM that initiates RI led to the identification of nonmuscle myosin heavy chain type II A and C as the self-targets in two different tissues. These results identify a novel pathway in which the innate response to a highly conserved self-antigen expressed as a result of hypoxic stress results in tissue destruction.

CORRESPONDENCE
Michael C. Carroll:
carroll@cbr.med.harvard.edu

Abbreviations used: ANOVA, analysis of variance; Hc, heavy chain; HRP, horseradish peroxidase; MBL, mannan-binding lectin; NMHC-II, nonmuscle myosin Hc type II; PARS, poly(ADP ribose) synthetase; PL, phospholipd; RI, reperfusion injury; ROS, reactive oxygen species; SPR, surface plasmon resonance.

Nucleated cells are highly sensitive to hypoxia, and even short periods of ischemia in multicellular organisms can have dramatic effects on cellular morphology, gene transcription, and enzymatic processes. Mitochondria, as the major site of oxygen metabolism, are particularly sensitive to changes in oxygen tension and during hypoxia release reactive oxygen species (ROS), which chemically modify intracellular constituents such as lipids and induce damage to DNA leading to cell injury and death (1, 2–5). In addition to endogenous intracellular events, ischemic tissue triggers an acute inflammatory response that enhances cell injury, resulting in necrosis. One current view is that ROS-modified structures formed during ischemia stimulate infiltration of inflammatory cells that mediate an acute inflammatory response leading to additional cell injury and death (6). However, this mechanism alone does not completely explain the acute nature of reperfusion injury (RI), because injury occurs even when inflammatory cells are limited (7, 8). Accumulating evidence supports a major role for the serum innate response, namely natural IgM and the complement system. Early observations that transient depletion of complement C3 reduced inflammation in a rat model of myocardial infarction suggested a role for innate immunity in RI (9). Subsequently, Weisman et al. demonstrated that pretreatment of rats with a specific soluble inhibitor of complement C3 (sCR1) dramatically reduced injury in a similar model of myocardial infarction and further established the importance of complement as a mediator of injury (10). Subsequent studies using the sCR1 inhibitor in various animal models, including porcine (11, 12) and mouse (13), and in various tissues as diverse as the central nervous system, intestine, or skeletal muscle confirmed and generalized the concept that the complement system was an important mediator of RI. Although the complete mechanism of injury is not clear, a role for the complement membrane attack complex (C5–C9) is supported by observations of deposition of complement C9 within reperfused heart tissues (14, 15), reduction in injury in mice deficient in C5 or treated with C5-specific antibody (16–19), and C6-deficient rabbits (20, 21). Importantly, RI injury in the skeletal muscle model is not only complement dependent but requires intact mast cells, as mice deficient in mast cell protease 5, one of the chymotryptic proteases found in granules, are protected from full injury (22).

The first indication that natural antibody was involved in initiation of RI derived from studies in mouse models bearing complete deficiencies in innate immune proteins such as complement components C3 and C4 and natural IgM. Results from these studies suggested that brief periods of ischemia led to an alteration in

surface epitopes, and this change resulted in binding by natural IgM and activation of the complement system (23, 24). Further support that specific natural IgM was involved followed from two separate reports that mice deficient in complement receptors CD21 and CD35 were protected in an intestinal model of RI despite a normal level of circulating IgM (25, 26). Reconstitution of the animals with pooled IgM (isolated from WT mice) or engraftment with WT peritoneal B-1 cells restored pathogenic IgM and RI. Notably, reconstitution of $Cr2^{-/-}$ mice with pooled murine IgG alone did not restore histological injury but enhanced neutrophil infiltration when combined with IgM (25). Most recently, identification of a single monoclonal IgM from a panel of B-1 cell hybridomas, which alone could restore injury in both intestine and hindlimb models of RI in antibody-deficient ($RAG\text{-}1^{-/-}$) mice, provided further support for the hypothesis that innate recognition of stress-induced self-antigens was involved in initiation of RI (27, 28).

In this paper, we identified a highly conserved region within nonmuscle myosin heavy chain (Hc) type II (NMHC-II) A and C as the target for natural IgM and initiation of injury in murine models of skeletal and intestinal RI. Five lines of evidence are provided that support a role for NMHC-II as the critical self-ligand in RI: (a) protein sequence analysis of natural IgM-bound NMHC-II isolated from lysates of RI tissue; (b) binding of NMHC-II by pathogenic IgM ($IgM^{CM\text{-}22}$) in an ELISA assay; (c) initiation of intestinal RI in $RAG\text{-}1^{-/-}$ mice with an anti–pan-myosin antibody; (d) sequence homology with a synthetic peptide isolated from phage display library that binds pathogenic $IgM^{CM\text{-}22}$ and blocks intestinal RI in WT mice; and (e) a synthetic peptide representing a conserved region of NMHC-II binds $IgM^{CM\text{-}22}$ in vitro and blocks RI in WT mice in two distinct tissues. Collectively, these results support the model that natural IgM recognition of NMHC-II expressed on the surface of ischemic tissue results in activation of the complement system and acute inflammation. These findings suggest a general mechanism by which stress, such as hypoxia, leads to expression of a highly conserved self-antigen on the cell surface and recognition by the innate immune system resulting in acute inflammation. These observations represent a clear example of the novel concept "innate autoimmunity" (29, 30).

RESULTS

Immune precipitation of self-antigens with natural IgM

The identification of a B-1 cell hybridoma clone ($IgM^{CM\text{-}22}$) that binds ischemic tissue in the murine intestinal and skeletal muscle models of RI provided support for the hypothesis that

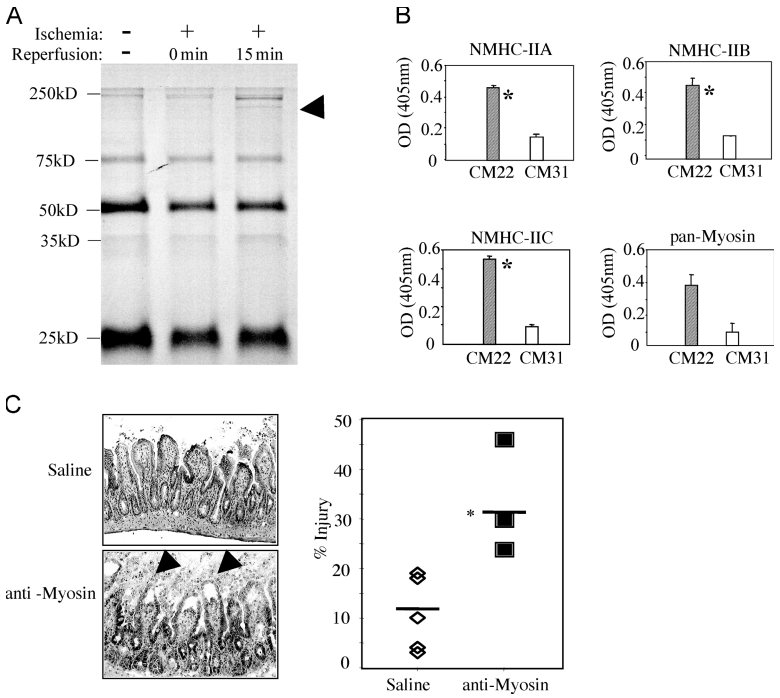

Figure 1. Immune precipitation of ischemia-specific antigens. (A) Detection of a unique band (arrowhead) at ~250 kD on SDS-PAGE (8%). Size markers are indicated on the left. Intestinal lysates were prepared from $RAG\text{-}1^{-/-}$ mice reconstituted with $IgM^{CM\text{-}22}$ and either sham control (no ischemia) or subjected to ischemia, followed by reperfusion for 0 or 15 min. (B) In vitro binding of $IgM^{CM\text{-}22}$ to NMHC-II. ELISA plates were coated with rabbit IgG antibodies specific for each of the three different isoforms of NMHC-II (top left, isoform A; top right, isoform B; bottom left, isoform C; or bottom right, anti–pan-myosin antibody). Bound myosin HC from intestinal lysates was detected by $IgM^{CM\text{-}22}$ or $^{CM\text{-}31}$. Results represent means ± SEM of OD 405 nm units and are representative of triplicate samples. (C) Anti–pan-myosin antibody restores RI in ischemic $RAG\text{-}1^{-/-}$ mice. $RAG\text{-}1^{-/-}$ mice were injected i.v. with saline (top left) or 50 µg of rabbit IgG anti–pan-myosin (bottom left), followed by RI treatment. (right) Scatter plot of pathology scores in which each symbol represents a single animal. *, $P < 0.05$.

ischemic tissue was altered relative to normal tissue and that neoepitopes expressed or exposed during ischemia were targets for an innate response to self (27, 28). Moreover, the availability of a specific IgM provided a means to identify the neoepitope. The rationale was that circulating IgM would bind self-antigens exposed during ischemia and that these complexes could be isolated and the antigens identified by proteomic techniques. RAG-$1^{-/-}$ mice were reconstituted with an optimal amount of IgM $^{CM-22}$, treated for intestinal ischemia, and reperfused for 0 or 15 min before harvesting of tissues. Immune complexes of IgM antigen were isolated from lysates of jejuneum at the two time points and fractionated by SDS-PAGE under reducing conditions. Analysis of the stained gels indicated common bands at varying molecular masses for all time points, including the sham control (Fig. 1 A). However, at 15 min an apparent unique band at high molecular mass (~250 kD) was identified (Fig. 1 A). Protein bands were excised from stained gels and enzymatically digested, and peptides were analyzed by tandem mass spectrometry as described previously (31). Analysis of eluted peptides indicated that the common bands at ~25, 50, and 75 kD represented immunoglobulin light chain and IgG and IgM Hc, respectively. The IgG Hc band at 50 kD was identified as goat and most likely represents Ig eluting from the beads, whereas the 75-kD band represents murine IgM Hc. Analysis of the high molecular mass band yielded peptide sequences homologous to NMHC-II isoforms A and C (Table I). In similar experiments using lysates prepared from WT mice treated for 3 h in intestinal RI, a similar size band at 250 kD was also observed and sequence analysis identified NMHC-II A and C peptides (unpublished data).

Three forms (A, B, and C) of NMHC-II have been identified in the mouse and human genomes (32, 33). All eukaryotic cells express NMHC-II, but the distribution of the three isoforms varies. NMHC-II A and B are ~85% homologous, whereas NMHC-II C is ~65% similar to A and B (32). The three isotypes are highly conserved among mice and humans. As a further test for binding of IgM $^{CM-22}$ to NMHC-II, an ELISA approach was followed. Plates were coated with antibody specific for each of the three forms of NMHC-II or with a pan-myosin antibody to capture the relevant antigen from lysates prepared from jejuneum of RAG-$1^{-/-}$ mice. Subsequently, IgM $^{CM-22}$ (or IgM $^{CM-31}$) was added and developed with a labeled anti–mouse IgM antibody. Above background binding of IgM $^{CM-22}$ but not IgM $^{CM-31}$ to all three of the isoforms of NMHC-II was observed (Fig. 1 B). The combined sequence analysis and ELISA results suggest that IgM $^{CM-22}$ recognizes a conserved region of the type II NMHC. As a further test of whether myosin is exposed to circulating antibody after ischemia, RAG-$1^{-/-}$ mice were reconstituted with a purified IgG fraction of rabbit anti–pan-myosin Hc. No evidence of rabbit IgG deposition was observed in tissues of reconstituted but sham-treated mice (unpublished data). In contrast, ischemic RAG-$1^{-/-}$ mice reconstituted with the myosin-specific IgG before reperfusion developed significant RI compared with saline controls (33 ± 11 vs. 11 ± 8; $P < 0.05$; Fig. 1 C). These results provide further support that myosin is exposed to antibody in circulation after ischemia. However, they did not identify the epitope within NMHC-II.

Table I. Tandem mass spectrometry results of isolated ischemic antigen

Matched proteins	Mass spectrometry (sequenced peptides)
Mouse NMHC-II A	VVFQEFR
(NP 071855;	CNGVLEGIR
total score = 130,	KFDQLLAEEK
peptides matched = 6)	KFDQLLAEEK
	EQADFAIEALAK
	QLLQANPILEAFGNAK
Mouse NMHC-II C	CNGVLEGIR
(AAQ24173;	VKPLLQVTR
total score = 133,	KFDQLLAEEK
peptides matched = 7)	KFDQLLAEEK
	EQADFALEALAK
	LAQAEEQLEQESR
	QLLQANPILEAFGNAK

Immunoprecipitations were performed as described in Materials and methods. Bands obtained from SDS-PAGE were digested and extracted for protein identification by tandem mass spectrometry. Peptides identified from the RI-specific 250-kD band were matched to isoforms A and C from NMHC-II. The Mascot score is defined as $-10 \times \text{Log}(P)$, where P is the probability that the observed match is a random event. Individual ion scores >53 indicate identity or extensive homology ($P < 0.05$).

Identification of an IgM $^{CM-22}$ ligand by phage display

As an alternative approach to identify the IgM $^{CM-22}$ target self-antigen, an M13 phage display library of random 12-mer amino acid sequences was screened with the specific IgM. After four rounds of positive selection with IgM $^{CM-22}$ and two rounds with negative selection with a control IgM (clone CM-75), 10 phage clones were isolated and the nucleotide sequence of the relevant M13 gene was analyzed. Notably, all 10 clones bore a codon sequence rich in asparagine. Four best binders to IgM $^{CM-22}$ were selected and one of these clones, P8 (which bound with the highest efficiency), was further characterized (Table II and Fig. 2 A). A 12–amino acid peptide (P8) was synthesized based on the phage sequence and assayed for inhibition of phage P8 binding to IgM $^{CM-22}$ (Fig. 2 B). Titration of increasing amounts of P8 peptide yielded 50% inhibition at an estimated concentration of 10–100 μM. This assay indicates a reasonable overall avidity of binding based on multiple binding sites expressed on the phage surface. This result also suggests that IgM $^{CM-22}$ binding to phage P8 is specific for the peptide region and that the synthetic peptide could be used as a mimetope for the actual antigen. To further characterize binding of P8 peptide to IgM $^{CM-22}$, ELISA plates were coated with the peptide and tested with varying concentrations of IgM $^{CM-22}$ or control IgM $^{CM-75}$ for binding (Fig. 2 C). At the lower concentration of 1 μg/ml, neither IgM bound above background. However, at 10 μg/ml significantly more IgM $^{CM-22}$ bound than IgM $^{CM-75}$ ($P < 0.05$).

Table II. Phage-displayed peptides bind to CM22 IgM and share conserved homology with NMHC-II

Peptides	Sequences
Phage clone	
P8	NGNNVNGNRNNN
Consensus	XNNNxNNxNNNN
NMHC-II	
Mouse-II A (542–556)	LMKNMDPLNDNI
human-II A (585–596)	LMKNMDPLNDNI
Mouse-II B (592–603)	LMKNMDPLNDNV
human-II B (592–603)	LMKNMDPLNDNV
Mouse-II C (607–619)	LMKNMDPLNDNV
human-II C (701–802)	LMKNMDPLNDNV
Control	AGC MPY VRI PTA

Peptides identified by screening phage display library with IgM $^{CM-22}$. Sequence of peptide region of phage clone P8 and consensus sequence based on 10 phage clones isolated from an IgM $^{CM-22}$–selected pool of M13 phage display library. Alignment of conserved regions of three isoforms of mouse and human NMHC-II is also provided. The corresponding amino acid positions in each isoform are listed in the parentheses. N2 peptide corresponds to the mouse and human NMHC-II C sequence.

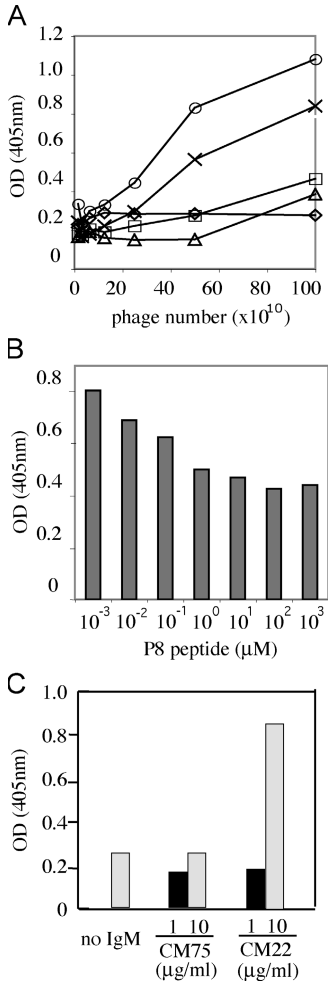

Figure 2. Screening of M13 phage display library identifies IgM $^{CM-22}$–specific peptides. (A) ELISA comparison of four phage clones isolated from an enriched pool IgM $^{CM-22}$–selected phage. Phage clone P8 binds with the highest relative efficiency (△, P1 clone; ×, P5 clone; □, P7 clone; ○, P8 clone; and ◇, control M13). Plate was coated with a solution of IgM $^{CM-22}$ before addition of varying concentrations of phage clones. (B) Synthetic peptide P8 inhibits IgM $^{CM-22}$ binding of phage clone P8. ELISA was performed with varying concentrations of synthetic P8 peptide added to an IgM $^{CM-22}$–coated plate before the addition of 5×10^{11} PFU phage. (C) ELISA assay for specific binding of P8 peptide to IgM $^{CM-22}$. Synthetic P8 peptide was coated on an ELISA plate followed by addition of saline, IgM $^{CM-75}$, or IgM $^{CM-22}$ at 1 (closed bar) or 10 (shaded bar) μg/ml. The bound IgM was detected by anti–mouse IgM-AP as described in Materials and methods. Results in A–C are representative of at least three independent experiments.

To test whether synthetic peptide P8 blocked IgM $^{CM-22}$ in vivo, antibody-deficient (RAG-$1^{-/-}$) mice were reconstituted with pathogenic IgM with or without the peptide. Previous studies had demonstrated that intestinal RI in RAG-$1^{-/-}$ mice was IgM-dependent and that IgM $^{CM-22}$ alone was sufficient to restore injury (24, 27). As expected, reconstitution of RAG-$1^{-/-}$ mice with IgM $^{CM-22}$ but not saline before reperfusion resulted in RI (Fig. 3, A [i] and B). In contrast, mixing of IgM $^{CM-22}$ with P8 peptide before injection in ischemic mice significantly blocked apparent injury (mean pathology score $= 6 \pm 3$ vs. 31 ± 13; $P < 0.001$; Fig. 3, A [ii] and B). Previous titration of peptide with IgM $^{CM-22}$ suggested that an optimal concentration of ~10 μM of peptide was sufficient to block 200 μg IgM $^{CM-22}$ (0.1–0.2 μM; unpublished data). Immunohistological analyses of serial sections of reperfused intestinal tissue (jejuneum) after RI identified colocalization of IgM and complement C4 and C3 within the microvilli in RAG-$1^{-/-}$ mice reconstituted with IgM $^{CM-22}$ but no deposition in sections prepared from mice receiving P8 peptide (unpublished data). No binding of IgM or complement was observed in IgM $^{CM-22}$–reconstituted sham controls, nor in RAG-$1^{-/-}$ mice reconstituted with control IgM $^{CM-31}$ or RAG-$1^{-/-}$ mice reconstituted with saline only (unpublished data) (27). Thus, peptide P8 appears to block binding of IgM $^{CM-22}$ and induction of injury in vivo.

To test whether peptide P8 represented a mimetope for a major self-antigen, WT mice were pretreated with peptide P8 (serum concentration of ~10 μM) 5 min before reperfusion in the intestinal model. Analysis of jejuneum tissues of mice treated with a similar concentration of control peptide or saline before reperfusion identified significant injury to the microvilli, as expected ($P < 0.05$; Fig. 3 A, iii). In contrast, pretreatment of WT mice with peptide P8 5 min before reperfusion blocked apparent injury relative to saline or control peptide (mean pathology score $= 5 \pm 3$ vs. 24 ± 16 and 23 ± 19, respectively; $P < 0.005$ and $P < 0.027$, respectively; Fig. 3, A [iv] and B). As expected, IgM, C4, and C3 colocalized within microvilli of RI-treated WT mice but not in mice administered P8 peptide (unpublished data). These results suggest that the number of key epitopes required to initiate RI is limited as a single peptide blocks injury and deposition of IgM and complement.

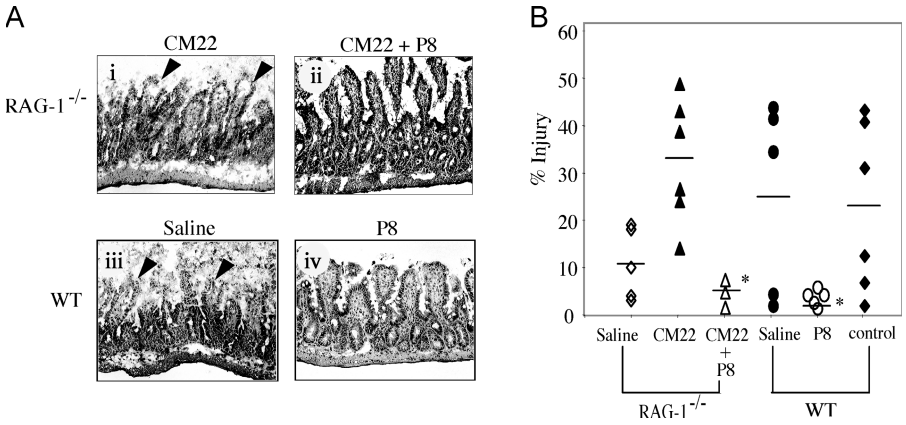

Figure 3. P8 peptide blocks RI in RAG-1$^{-/-}$ mice and WT animals. (A, i and ii) Representative sections (stained with hematoxylin and eosin) prepared after RI treatment in RAG-1$^{-/-}$ mice with IgM $^{CM-22}$ alone or mixed with P8 peptide, respectively. (iii and iv) Representative sections prepared from WT mice and treated for intestinal RI that received either saline or P8 peptide 5 min before reperfusion. Arrowheads indicate pathologic features of injury. Magnification, 200. (B) Scatter plot indicates mean pathology score of each group of treated animals. Each symbol represents one animal. Control group is WT mice pretreated with a control peptide (AGCMPYVRIPTA) at a similar dose of P8 peptide. *, $P < 0.05$ as determined by Student's *t* test of the P8 treated versus untreated groups.

Identification of self-peptide that binds IgM $^{CM-22}$

Comparison of the sequences of the three NMHC-II isoforms with the P8 peptide sequence identified one region of apparent homology (Table II). All three isoforms include a motif of NxxxxNxNx that suggested similarity with the P8 sequence. A 12–amino acid synthetic peptide (referred to as N2) sequence (represents the NMHC-II C isoform) was prepared for further study. To test whether this region bound to IgM $^{CM-22}$, surface plasmon resonance (SPR) analysis was used (Fig. 4). N2 peptide was injected over a surface coupled with IgM $^{CM-22}$ (Fig. 4 A) and generated a robust response, which corresponded to a KD of 123 ± 61 μM (mean ± SD; $n = 2$) as calculated from the steady-state response levels (Fig. 4 C). In contrast, no binding was observed when a control peptide was injected over the specific IgM-coupled surface (Fig. 4 B) or when the N2 peptide was injected over a surface coupled with the IgM $^{CM-31}$ control IgM (Fig. 4 D).

Self-peptide blocks intestinal RI injury

To test whether NMHC N2 peptide represents the major self-epitope in intestinal RI, WT mice were treated with saline or increasing concentrations of the synthetic peptide (final serum concentrations = 8, 16, 32, or 40 μM, respectively) 5 min before reperfusion in the intestinal model. Histological analysis of tissue sections of saline-treated WT mice identified injury that correlated with deposition of IgM and complement as expected (Fig. 5, A [i], B, and D [i–iv]). In contrast, treatment of WT mice with an increasing concentration of N2 peptide demonstrated a dose-dependent reduction in injury (mean pathology scores: saline, 22 ± 17% [$n = 9$]; 8 μM, 21 ± 7% [$n = 3$; $P < 0.40$]; 16 μM, 17 ± 5% [$n = 3$; $P < 0.20$]; 32 μM, 8 ± 6% [$n = 3$; $P < 0.03$]; and 40 μM, 7 ± 4% [$n = 7$; $P < 0.01$]) (Fig. 5, A [ii] and B). Thus, significant protection from injury was achieved with 32- and 40-μM concentrations of N2 peptide. Interestingly, P8 peptide was protective at a lower concentration (10 μM), correlating with its higher CM-22 binding affinity relative to N2.

To further evaluate the protection by N2 peptide, mice were characterized for intestinal permeability. In this assay mice are administered horseradish peroxidase (HRP) enterally 10 min before ischemia, and uptake into circulation is

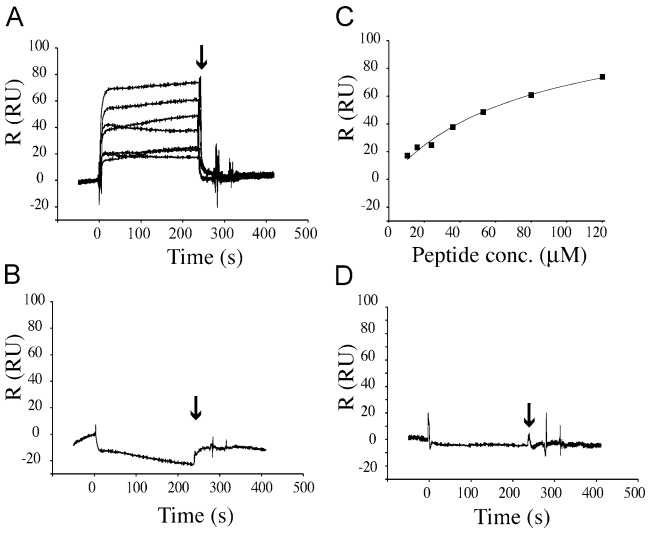

Figure 4. SPR. (A) Binding isotherms for samples of the N2 peptide with concentrations from 10.5 to 120 μM injected over the IgM $^{CM-22}$–coupled surface. (B) Binding isotherm for a same-length random sequence control peptide (AGCMPYVRIPTA) injected at a concentration of 117 μM over the IgM $^{CM-22}$–coupled surfaces. (C) Nonlinear curve fitting with a 1:1 Langmuir binding isotherm to the steady-state response levels for the injection showed in A ($\chi^2 = 10$). (D) The binding isotherm for the injection of the N2 peptide at 120 μM over a surface coupled with control IgM $^{CM-31}$. In A, B, and D, the injection phases had a duration of 240 s each, with the ends of the injection marked by arrows.

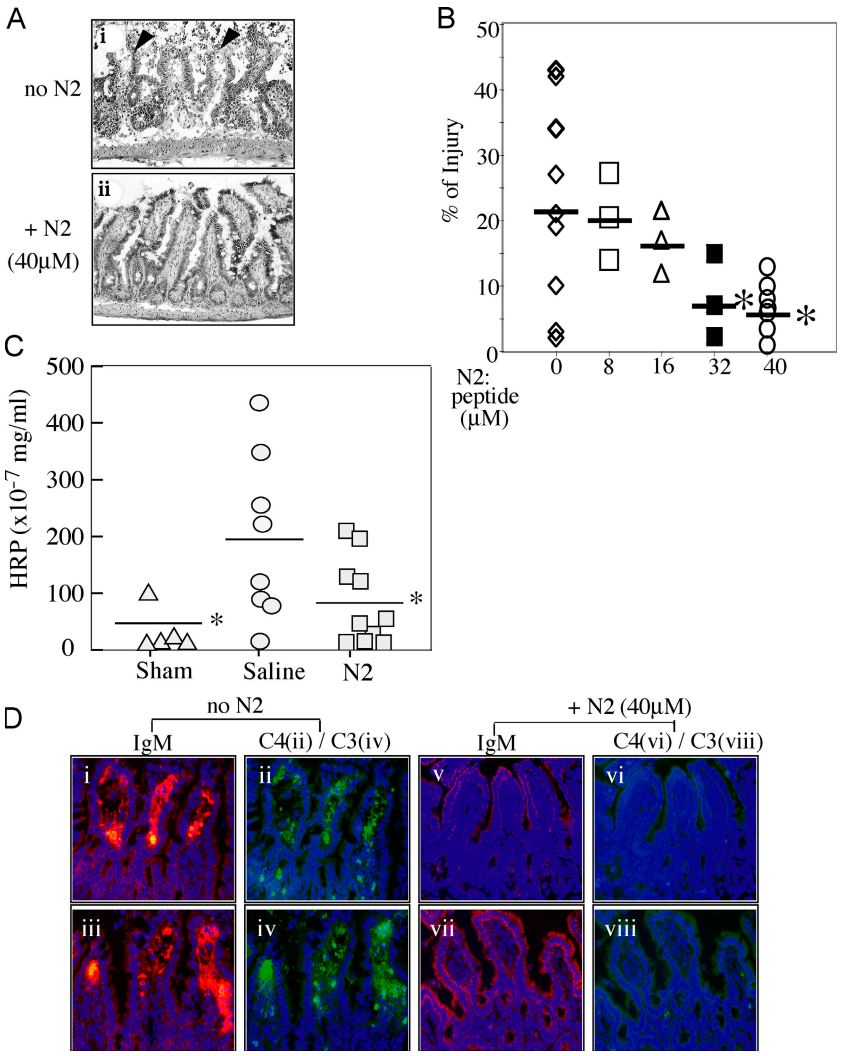

Figure 5. Treatment of mice with NMHC-II N2 peptide blocks intestinal RI. (A) Representative sections prepared from WT mice treated for intestinal RI and injected i.v. with either saline (i) or 40 μM N2 peptide (ii) 5 min before reperfusion. (B) Scatter plot indicates mean pathology score of each group of treated animals. WT mice were injected with saline or varying concentrations (final serum concentrations of N2 are indicated) of N2 peptide 5 min before reperfusion. Each symbol represents a single mouse. *, $P < 0.05$ as determined by Student's *t* test. (C) Scatter plot indicates mean plasma levels of 40-kD HRP of each group of treated animals 3 h after reperfusion. WT mice were administered HRP by gavage 10 min before the induction of intestinal RI and further treated with control, saline, or 40 μM N2 peptide 5 min before reperfusion. Each symbol represents a single mouse. *, $P < 0.05$, based on Student's *t* test. (D) 32 and 40 μM N2 peptide blocks IgM binding and activation of complement in intestinal RI. Representative cryosections of intestinal tissues were harvested after intestinal RI and treated with antibodies specific for mouse IgM, C4, or C3. Magnification, 400. Results are representative of at least five experiments. Immunohistology was not performed on tissues harvested from mice treated with the lower doses of peptide. WT mice were without N2 (i–iv) or pretreated with N2 (v–viii). (i, iii, v, and vii) Sections were stained with anti-IgM–biotin, followed by streptavidin–Alexa 568 (red), and counterstained with DAPI (violet). Sections in panels ii and vi were stained with anti-C4–FITC (green), and the sections in panels iv and viii were stained with anti-C3–FITC (green).

measured after RI treatment. Hart et al. recently reported using a similar assay to measure intestinal permeability in RI-treated mice but administered FITC–dextran (34). Our results indicate significant uptake of HRP into circulation in WT mice treated with saline versus sham controls (195.4 ± 51.7 vs. 31 ± 17.3 [$n = 8$ and 5, respectively]; $P < 0.05$; Fig. 5 C). In contrast, mice pretreated with an optimal amount of N2 peptide before reperfusion develop significantly less permeability than saline-treated mice (79.8 ± 30 vs. 195.4 ± 51.7 [$n = 10$ and 8, respectively]; $P < 0.05$; Fig. 5 C). Thus, pretreatment of mice with N2 peptide protects from both histological injury and intestinal permeability.

Protection from injury correlated with a reduction in deposition of IgM and complement in mice treated with 40 μM N2 peptide (Fig. 5 D, v–viii). Notably, among the control mice not all animals developed full injury even though treatment with N2 (or P8) peptide gave substantial protection. We speculate that the range in injury observed among WT

mice is caused by a variation in serum levels of specific natural IgM because this pattern is not observed in RAG- $1^{-/-}$ mice treated with IgM $^{CM\text{-}22}$ (Fig. 3). Moreover, IgM and complement deposition correlate with the level of injury; i.e., WT mice with a low injury score have low level of IgM (unpublished data).

Previous reports identified vascular permeability of labeled albumin as a measure of severity of intestinal RI (23, 26, 27). To evaluate further the effects of treatment with N2 peptide in the intestinal RI model, we used an intravital approach combined with a novel miniaturized laser scanning confocal microscope to image leakage of microvessels within the villi of the jejunum. In this approach anesthetized mice are administered a fluorescent-labeled vascular probe (AngioSense 680) that circulates within normal blood vessels for up to 2 h. Besides its stability in circulation, an advantage of this novel probe is that it emits in the near infrared and, thus, imaging is in the low energy range. To image circulation within the microvilli, a scanning confocal stick lens (approximately the diameter of a biopsy needle) is inserted within a small incision in the wall of the jejuneum and placed in direct contact with the mucosal surface. Contrast is provided by pretreatment of mice i.v. with Rhodamine 6G, which is taken up by cells, especially the enterocytes lining the microvilli. Mice are injected with the vascular probe 5 min before reperfusion, and imaging is initiated 15 min after reperfusion. For example, among the sham controls, the blood vessels within the lamina propria of microvilli are identified by the circulating vascular probe (red), which is contrasted by the green stain of the enterocytes (Rhodamine 6G; Fig. 6 A, i). In experimental mice, significant leakage of the vascular probe is observed as early as 20 min after reperfusion, as indicated by the presence of red dye within the lamina propria and surrounding target tissues. The mean ratio of vessel (V) to background (B) is 149 ± 14 versus 16 ± 4 in arbitrary units for sham controls and saline-treated mice, respectively ($P < 0.001$; Fig. 6, A [ii] and B). In contrast, limited leakage of the vascular probe was observed in experimental mice pretreated with N2 peptide (153 ± 4 vs. 149 ± 14 units for N2- and saline-treated mice, respectively; $P < 0.001$; Fig. 6, A [iii] and B). Thus, administration of an optimal amount of N2 peptide 5 min before reperfusion effectively limited leakage of the vascular probe.

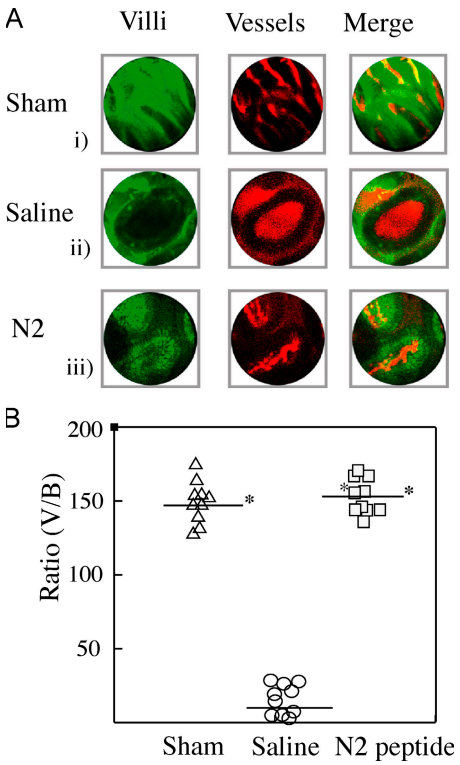

Figure 6. N2 peptide blocks vascular leak in intestinal RI. (A, i–iii) Representative images of microvilli within the jejuneum of sham, saline, or N2 administered mice, respectively. Mice were treated for RI as described in Fig. 5, except that 5 min before reperfusion the later two groups were injected i.v. with a mixture of vascular probe (AngioSense 680, red) and Rhodamine 6G (green) in saline or N2 peptide (40 μM final concentration). (i) Results of the sham group identify microvasculature of individual microvilli in which red indicates blood vessels and green outlines enterocytes and lamina propria. (ii) Saline group images indicate extensive leakage of the vascular probe into lamina propria and surrounding tissues. (iii) N2 peptide group results indicate relatively normal vasculature within microvilli and limited leakage of vascular probe. (B) Scatter plot of ratio of intensity of signal of vessels (V) versus background (B). The horizontal lines indicate the mean of samples analyzed. Each symbol indicates a representative measurement from representative images of at least three mice per group, and means ± SD were calculated. *, $P < 0.001$, as determined by Student's *t* test.

Self-peptide blocks RI injury in skeletal muscle

The identification of a single self-peptide that blocks intestinal RI in WT mice led to the general question of whether the N2 region of NMHC-II was also the target for pathogenic IgM among other ischemic tissues. It might be predicted that the number of antibodies specific for ischemic tissue is limited based on the current understanding that the repertoire of natural IgM is relatively small (35–37) and putatively selected through evolution (38, 39). Moreover, ligands of natural IgM are considered highly conserved structures and are probably limited in number.

To test whether NMHC-II represents the self-ligand target in the murine hindlimb model, mice were treated for 2 h of ischemia followed by 3 h of reperfusion as described previously (28). As expected, WT mice administered saline or 40-μM control peptide (Table II) developed considerable injury. In contrast, injury was significantly reduced in mice administered 40 μM (final serum concentration) of N2 peptide before reperfusion (mean number of injured muscle fibers per 50 counted = 25 ± 4 and 22 ± 3 for saline and control peptide, respectively, vs. 12 ± 1 for N2 treated; $P < 0.01$ and $P < 0.05$, as determined by Student's *t* test between saline and control peptide and N2 and control peptide, respectively; $P < 0.05$ for all groups, as determined by analysis of variance [ANOVA]) (Fig. 7, A and B). Thus, these results suggest that, as in the intestinal model, NMHC-II is the major self-ligand in ischemic skeletal muscle.

DISCUSSION

The recent identification of a natural antibody (IgM $^{CM-22}$) that initiates intestinal and skeletal muscle RI in antibody-deficient mice has provided an important reagent to isolate and characterize the self-antigen involved in initiation of acute inflammation (27, 28). In this paper, we provide five lines of evidence that support the identification of the self-antigen as a highly conserved region (represented by N2 peptide) within NMHC-II. Notably, pretreatment of WT mice with N2 peptide (or the mimetope P8) after ischemia but before reperfusion dramatically reduced RI within both intestinal and skeletal muscle models.

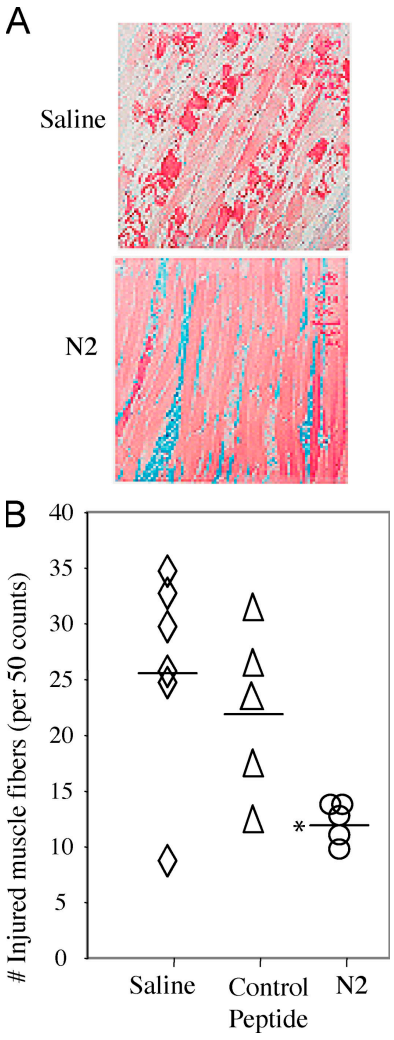

Figure 7. N2 peptide is protective in skeletal muscle model of RI. WT mice were treated in the hindlimb model of RI and administered either saline, control, or N2 peptide before reperfusion. (A) Representative sections of hindlimb muscle isolated from mice pretreated with either saline (top) or 40 μM N2 peptide (bottom). Samples were stained with Masson's Trichrome for histology. Magnification, 200. (B) Injury score based on the percentage of injured fibers per 50 counted. Each symbol represents a single mouse. *, $P < 0.05$ as determined by Student's *t* test between N2 and control peptide; $P < 0.01$ as determined by Student's *t* test between N2 and saline; and $P < 0.05$ as determined by ANOVA for all groups.

15 types of myosin Hc have been identified to date. Like other myosins, the NMHC-II form hexamers of two Hc (~250 kD each) and two pair of regulatory light chains (20 and 17 kD each). Functionally, they all bear ATPase activity, form molecular motors within the cell, and are thought to be important in regulating cytokinesis, cell motility, and cell polarity (40). Of the three isoforms, little is known of the functional importance of the recently identified NMHC-II C.

Studies in cell culture and in isolated hearts made ischemic and reperfused in the absence of blood cells or sera reveal evidence of cell injury to cardiomyocytes, suggesting that factors independent of inflammation can lead to cell injury (2, 41). One well-characterized pathway is poly(ADP ribose) synthetase (PARS), which is a nuclear enzyme involved in DNA strand break repair (3). Damage to chromatin by free radicals resulting from ROS, which form during hypoxia, leads to activation of PARS that has multiple effects, including depletion of mitochondrial ATP and eventual cell injury. Although the effects of hypoxia on NMHC-II have not been reported, one possible link with generation of ROS and activation of the PARS pathway is that nonmuscle myosins, which are involved in maintaining cell morphology, migrate to the outer membrane after cell injury (42). Thus, a general explanation for the combined pathways is that NMHC-II is mobilized to the cell surface by hypoxia-related events resulting in transient exposure of the N2 region on the outer cell surface of endothelium and muscle cells. This exposure would provide a target for circulating pathogenic IgM resulting in enhancement of cell injury beyond that caused by endogenous intracellular pathways such as PARS. We propose that the NMHC-II epitope is exposed on hypoxic cells and not released as a result of cell death. If the latter were the case, multiple other self-antigens would be released and also serve as targets for circulating natural IgM, which binds many intracellular antigens. Based on the direct visualization of vascular leakage, it seems most probable that injury is initiated at the endothelium surface.

Expression of novel cell surface molecules in response to stress is not unprecedented, although examples are generally based on in vitro study. For example, a recent report identified mouse and human NKG2D ligands up-regulated in nontumor cell lines by genotoxic stress and stalled DNA replication (43). In their in vitro model, expression of the novel NK receptor ligands was dependent on the ataxia telangiectasia, mutated pathway. Thus, they propose "a novel link between the immune response and processes that regulate genome integrity" (43). Alternatively, in our system, NMHC-II could be released into circulation or the extracellular space and bound by antibody. Attempts to measure specific release of NMHC were unsuccessful to date. As more specific reagents are developed, it will be important to identify the kinetics of exposure/release by hypoxic cells. Thus, in the absence of IgM as in RAG-$1^{-/-}$ mice or peptide blocking of IgM with N2 or P8, we speculate that cell injury is reversible

at least within the conditions of ischemia used in the current experiments. Of course, prolonged hypoxia would lead to irreversible cell injury and cell death independent of the innate immune system.

Although our experiments suggest that NMHC-II is the major antigen exposed during reversible RI, other epitopes are likely exposed on the surface of injured endothelium but in the absence of specific natural IgM are insufficient to mediate inflammation. Support for additional antigens comes from recent reports by Fleming et al.(44, 45). Using a similar model of mesenteric RI, they reported that murine and human antibodies specific for phospholipids (PLs) and/or β-2 glycoprotein could restore injury in $Cr2^{-/-}$ or RAG-$1^{-/-}$ animals. Because the murine anti-PL and β-2 antibodies are of the IgG subclass and were isolated from autoimmune mice (NZW × BxSB F1), they likely represent high-affinity antibodies that arose as a result of autoimmune disease. Similarly, IgG antibodies from 5-mo-old but not 2-mo-old B6.MRL/lpr autoimmune-prone mice are pathogenic in RI-treated RAG-$1^{-/-}$ mice. Whether natural IgM of similar specificity occur in nonautoimmune animals is unclear. However, given that pretreatment of WT mice with N2 or P8 peptides blocks injury in our two models, antibodies specific for self-antigens, such as PL or β-2 glycoprotein I, are not likely involved in the initiating event. However, after induction of RI it is clear that many additional self-antigens are released and become targets for self-specific natural IgMs. This could explain the observation by Fleming et al. (45) that mesenteric ischemic in the B6.MRL/lpr strain is more severe than WT controls as they express a higher level of self-reactive antibodies of both IgM and IgG subclasses (46).

The pharmokinetics of N2 peptide are yet to be completely elucidated, but an initial serum concentration of ~32–40 μM is sufficient to block substantial injury in ischemic RAG-$1^{-/-}$ mice administered IgM $^{CM\text{-}22}$ or WT mice over the 3 h of reperfusion. Because the peptide likely has a very short half-life in serum, it either binds with sufficient high affinity to the IgM to inhibit recognition of ligand over the complete period of reperfusion, or the ligand is only exposed transiently on reperfusion and peptide is only required after initial reperfusion. The kinetics of peptide binding determined by Biacore assay suggest that the former is unlikely and, therefore, we favor the latter possibility. Earlier studies in a rat myocardial RI model identified increased myocardial injury 7 d after ischemia (10). Injury was complement dependent, as pretreatment with a soluble inhibitor of C3 considerably reduced late injury. A limitation of the intestinal model is that injured microvilli are replaced by newly migrating enterocytes that emanate from stem cells in the crypts (47). Although it seems likely that pretreatment with peptide will block late injury as it does acute, these studies will be important to follow up in the skeletal or cardiac muscle models.

Given the highly conserved nature of the N2 region, it is possible that exposure of other forms of myosin Hc, such as smooth muscle, could also serve as a target for natural antibody. However, it is notable that only NMHC-II A and C isoforms were identified in the immune precipitation analyses, suggesting that these are the major antigens exposed/expressed during ischemia, at least in the intestine. It will be important to characterize the IgM–self-antigen complexes in the hindlimb model. Natural IgM, which is a product of innate lymphocytes (i.e., B-1 cells), is considered a component of innate immunity because of its germ line–encoded repertoire, absence of somatic mutation, and specificity for structures highly conserved among both prokaryotes and eukaryotes (35–38). Therefore, it is not surprising that a highly conserved region of myosin could also serve as a target for natural IgM.

It is proposed that natural antibody recognition of the N2 epitope is conserved among vertebrates, as identified for other B-1 cells such as for T-15 specificity. Natural IgM of the T-15 specificity binds oxidized lipids and phosphoryl choline (38). Moreover, like anti–phosphoryl choline natural IgM, the serum levels of N2-specific antibody probably also vary among mice. If so, it will be important to test whether N2-specific antibody levels correlate with susceptibility to RI. Furthermore, we propose that this innate response to a stress-induced self-antigen represents a general mechanism referred to as "innate autoimmunity" (29, 30). This novel concept was recently proposed to explain a role for Toll-like receptors in mediating sterile inflammation in response to self-ligands (29). Our observation that a natural antibody recognizes a highly conserved self-antigen, resulting in sterile inflammation and tissue destruction, extends this notion to other pathways of innate recognition. Although a response to NMHC-II by Toll-like receptors was not examined, it is possible that they could participate in a secondary role as cells dying as a result of inflammation release other potential self-ligands. Similarly, other components of innate recognition such as mannan-binding lectin (MBL) (48), surfactants (49, 50), and C1q (51), which are known to bind and clear apoptotic cells, could play a secondary role after cell injury. Recently, Hart et al. reported the novel observation that injury in a mesenteric model of RI is dependent on MBL and complement C2 but not C1q (34). Based on the importance of IgM and C4, it was assumed that injury was mediated via the classical pathway. We propose that IgM initiates the lectin pathway based on preliminary experiments indicating IgM deposition but an absence of C4 or C3 binding in MBL-a/c double-deficient mice (unpublished data). Thus, recognition of NMHC-II and deposition of IgM either facilitates binding of MBL to IgM or exposes an MBL binding site on ischemic tissue leading to its activation.

RI represents a major health problem because it affects most tissues, including the intestine, myocardium, and central nervous system, and at present there are no effective therapies or treatment (52). Intestinal ischemia, particularly the acute form, has a high mortality rate (70–90%) (53). The identification of a common epitope that is conserved among vertebrates and represents the target for natural IgM in a murine model of RI could provide a basis for development of a new category of therapeutics. Indeed, our finding that N2

peptide inhibits RI in two distinct tissues supports the feasibility of the approach.

In summary, we have identified a conserved region of myosin Hc that serves as the target for natural IgM in two murine models of RI. It is proposed that this pathway represents a novel response by the innate immune system to self-antigens induced by hypoxia or other forms of cell stress.

MATERIALS AND METHODS

Phage display peptide library and peptide synthesis. A 12-mer M13 phage display library (New England BioLabs, Inc.) was screened for four rounds with MBL beads coated with IgM $^{CM-22}$ and counterselected by one round of rat IgM followed by one round of IgM $^{CM-75}$, according to the manufacturer's recommendation. Phage clones were selected from the enriched pool, and the nucleotide sequence of the relevant phage gene was determined for <10 clones. Selected peptides were synthesized with a purity >95% in the Harvard Proteomic Core or New England Peptide, Inc.

Binding assays. ELISA was performed as described previously (27). In brief, IgM binding to phage or phage-specific peptides was determined by coating a 96-well plate with saturating amounts of antigen. Subsequent to blocking, 1 or 10 μg/ml IgM was added for 2 h at 37°C. Plates were washed and developed with alkaline phosphatase–labeled goat anti–mouse IgM (Sigma-Aldrich). To detect binding of IgM to NMHC-II, plates were coated with specific rabbit IgG, and fresh intestinal lysate was added as a source of antigen. Subsequently, plates were washed, a source of natural IgM (i.e., IgM $^{CM-22}$ or IgM $^{CM-31}$) was added, and binding was detected as described in the previous sentence. The following rabbit antibodies were used: NMHC-II A and B (Covance Inc.), NMHC-II C (a gift from R. Adelstein, National Institutes of Health [NIH], Bethesda, MD), and pan–myosin Hc (Sigma-Aldrich). Lysates were prepared as described in Immune precipitation.

Intestinal RI model. RAG-$1^{-/-}$ and C57BL/6 mice used in this study were purchased from Jackson ImmunoResearch Laboratories and maintained within the mouse colony under specific pathogen-free conditions at Harvard Medical School according to NIH guidelines on animal welfare. Procedures involving animals were approved by the Institutional Review Boards at the CBR Institute, Harvard Medical School, Massachusetts General Hospital, and Brigham and Women's Hospital. Surgical protocol for RI was performed as previously described (27). In brief, a laparotomy is performed, a microclip (125 *g* pressure; Roboz) is applied to the superior mesenteric artery, and bilateral circulation is limited with silk sutures flanking a 20-cm segment of the jejuneum. After 40 min of ischemia, the microclip was removed, and reperfusion of the mesenteric vasculature was confirmed by the return of pulsation to the vascular arcade and a change to pink color. The incision was closed, and all animals were kept warm for 3 h. Reconstituted RAG-$1^{-/-}$ animals received either IgM mixed with peptide or saline in 0.2 ml volume i.v. 30 min before the initial laparotomy. WT animals were treated with saline or peptide i.v. 5 min before reperfusion. At the end of reperfusion, the ischemic segment of the jejunum was harvested, and the central 4 cm was cut for pathological analysis.

Hindlimb RI model. 8–12-wk-old WT mice underwent 2 h of hindlimb ischemia and 3 h of reperfusion as previously described (28). In brief, bilateral rubber bands (Latex O-Rings; Miltex Instruments) were applied above the greater trochanter. Rubber bands were removed, and limb reperfusion was confirmed by return of pink color. Tissues were fixed for 8 h in 4% paraformaldehyde and sectioned for Masson's Trichrome staining. 50 individual muscle fibers were counted per section, and the injury was reported as the number of damaged fibers per 50 fibers counted.

Histopathology and immunohistochemistry analysis. Cryostat sections of intestinal tissues were stained by hematoxylin and eosin and examined by light microscopy for mucosal damage. Pathology score was assessed based on a procedure modified from Chiu et al. (54) that included direct inspection of all microvilli over a 4-cm stretch of jejuneum, as described previously (27). In brief, the integrated injury score = $S/(V + [P \times 25]) \times 50\% + D/(V + [P \times 25]) \times 100\% + (P \times 25)/(V + [P \times 25]) \times 100\%$, where V = total number of villi; S = villi appearing with subepithelial space, defined as an acellular space under a continuous epithelial layer and a milder form of damage; D = villi appearing with epithelial disruption, defined as discontinuation of an epithelial layer of villus and a more severe form of damage; and P = villi lost over the length of intestine measured using a 100× field (each field has an average of 25 jejunal villi; thus, by aligning the intestinal wall through the center of each power field, an estimate of the number lost can be made). For immunofluorescence, cryosections fixed with 4% (wt/vol) paraformaldehyde were incubated for varying periods with biotin-labeled anti–mouse IgM (Becton Dickinson), followed by 1 h with streptavidin–Alexa 568 (Invitrogen). C4 deposition was detected by staining with FITC-labeled rabbit anti-huC4c (DakoCytomation), followed by anti–rabbit–Alexa 488 (Invitrogen). The specificity of anti-C4c staining was confirmed by staining serial sections with biotin-labeled anti–mouse C4 for 1 h followed by streptavidin–FITC (Becton Dickinson). C3 deposition was detected by treating with FITC-labeled anti-C3 (DakoCytomation). Sections were mounted in antifade mounting medium with DAPI (Invitrogen).

SPR analysis of peptide binding to antibody. IgM (IgM $^{CM-22}$ or $^{CM-31}$) antibody was immobilized by amine coupling in a chip (SPR CM5; Biacore) flowcell at a density of 33,400 response units per ~33 ng/mm^2 as described previously (55). A reference flow cell was prepared by coupling of ethanolamine-HCl. Peptides, diluted in PBS running buffer, were flowed separately over the IgM-coupled surface and the reference at a rate of 10 μl/min at 25°C, with the data collection rate at 10 Hz. The injection phase had a duration of 240 s (the ends of injection phases are marked by arrow heads). Binding isotherms were derived by subtracting the response in the reference cell from the response of the IgM-coupled surface. After each run, the surface was regenerated by injecting 40 μl 0.05% (vol/vol) polyoxyethylenesorbitan monolaureate/PBS.

Immune precipitation. Frozen tissues were homogenized in a lysis buffer containing detergent and a cocktail of enzyme inhibitors. A sample of lysate is analyzed for total protein content (protein assay dye; Bio-Rad Laboratories) to ensure similar levels of protein for analysis. Lysates are mixed with sepharose beads coated with rat anti–mouse IgM for 1 h at 4°C. Subsequently, beads were pelleted gently, washed in lysis buffer, and boiled in SDS sample buffer under reducing conditions to elute bound complexes. Samples were fractionated on 8% (wt/vol) polyacrylamide SDS gels and subsequently fixed and stained with either Coomassie blue or silver stain to identify protein bands.

Protein identification by tandem mass spectrometry. Individual Coomassie-stained bands were excised from SDS gels, destained, and subjected to enzyme digestion as described previously (56). The peptides were separated using a nanoflow liquid-coupled chromatography system (CapLC; Waters), and amino acid sequences were determined by tandem mass spectrometer (Q-Tof micro; Waters). Mass spectrum (MS)/MS data were processed and subjected to database searches using Mascot (Matrix Science) against the UniProtKB/Swiss-Prot, TrEMBL-NEW, or the NCBI nonredundant databases.

Intestinal permeability. Intestinal permeability was determined by measuring the appearance of HRP in blood (molecular mass = 40 kD; Sigma-Aldrich) administered by gavage as described previously (57). The model used for investigating intestinal permeability was basically identical to the surgical protocol described in Intestinal RI model, except bilateral circulation limitation with silk sutures was not performed to maintain an open lumen during the study. In brief, 10 min before intestinal RI was induced, mice were administered 10 μl/g body weight of phosphate-buffered saline

(pH 7.4) containing 2 mg/ml HRP by gavage. To test the blocking effect of N2 peptide in intestinal RI, WT C57BL/6 mice were treated with saline or peptide (final serum concentration = 40 μM) in a volume of 100 μl i.v. 5 min before reperfusion. Blood samples were obtained in a capillary tube 3 h after reperfusion by retroorbital puncture. Blood samples were allowed to clot overnight at 4°C and centrifuged (3,000 rpm) for 10 min. Serum samples were diluted and added to a 96-well microplate (Nalge Nunc) precoated with goat anti-HRP antibody (1:2,500 dilution; Sigma-Aldrich). The plate was then incubated for 2 h at 37°C, after which the wells were washed three times with phosphate-buffered saline (pH 7.4) and 0.1% Tween 20. HRP activity was determined by adding 100 μl of reagent (TMB One-Step Substrate System; DakoCytomation) for 15 min, and the reaction was stopped with 100 μl 2N H_2SO_4. The concentration of HRP was determined by spectrometry at 450 nm.

Vascular leakage. Leakage was determined in real time using an intravital imaging approach combined with a novel scanning laser confocal microscope (prototype scanner from Olympus Corp.) and a vascular probe (AngioSense 680; VisEn Medical) as described previously (58). Mice were anesthetized with a 0.3-ml i.p. injection of 15 mg/ml ketamine Hcl and 3 mg/ml xylazine and injected i.v. with AngioSense 680 (10 nmol/mouse) and Rhodamine 6G (Invitrogen) 5 min before reperfusion. Mice treated for intestinal RI (see Intestinal permeability) and sham controls were prepared for imaging before reperfusion by making a small incision within the wall of the exposed jejuneum and inserting the "stick-lens" (1.3 mm diameter) of the prototype confocal setup. Imaging of the microvilli was initiated 15 min after reperfusion and continued for up to 45 min. Images were prepared at varying time points after reperfusion. Results from representative images of the three groups of mice (i.e., sham, saline, and N2 peptide) were analyzed by imaging software (Image J version 1.34; Wayne Rasband, NIH, Bethesda, MD) by taking 10 measurements of representative fields of view, and the intensity of red dye within the target vessels (V) versus surrounding background (B) tissue was determined. Results were calculated as ratio of V/B intensity ± SD.

Statistical analysis. Data in all figures (except Fig. 6, in which SD is used) are expressed as means ± SEM. Statistical comparisons between groups were made by Student's *t* test, and ANOVA was used for comparisons of multiple groups. $P < 0.05$ was considered significant.

We thank Drs. Robert Adelstein and James Sellers, Jules Hoffmann, and Mark Entman for helpful discussions and critical comments and Dr. Robert Adelstein for the gift of reagents.

Research was supported by grants P50 GM52585 (to M.C. Carroll and F.D. Moore) and R44 AI051045 (to E.M. Alicot) from the NIH.

M.C. Carroll and F.D. Moore both consult and, along with E.M. Alicot, own shares in DecImmune Therapeutics. The authors have no other conflicting financial interests.

Submitted: 22 February 2005
Accepted: 2 December 2005

REFERENCES

1. Wu, B., A. Ootani, R. Iwakiri, T. Fujise, S. Tsunada, S. Toda, and K. Fujimoto. 2004. Ischemic preconditioning attenuates ischemia-reperfusion-induced mucosal apoptosis by inhibiting the mitochondria-dependent pathway in rat small intestine. *Am. J. Physiol. Gastrointest. Liver Physiol.* 286:G580–G587.
2. Thiemermann, C., J. Bowes, F.P. Myint, and J.R. Vane. 1997. Inhibition of the activity of poly(ADP ribose) synthetase reduces ischemia-reperfusion injury in the heart and skeletal muscle. *Proc. Natl. Acad. Sci. USA.* 94:679–683.
3. Szabo, G., L. Liaudet, S. Hagl, and C. Szabo. 2004. Poly(ADP-ribose) polymerase activation in the reperfused myocardium. *Cardiovasc. Res.* 61:471–480.
4. Becker, L.B. 2004. New concepts in reactive oxygen species and cardiovascular reperfusion physiology. *Cardiovasc. Res.* 61:461–470.
5. Becker, L.B., T.L. Vanden Hoek, Z.H. Shao, C.Q. Li, and P.T. Schumacker. 1999. Generation of superoxide in cardiomyocytes during ischemia before reperfusion. *Am. J. Physiol.* 277:H2240–H2246.
6. Li, C., and R. Jackson. 2002. Reactive species mechanisms of cellular hypoxia-reoxygenation injury. *Am. J. Physiol. Cell Physiol.* 282: C227–C241.
7. Briaud, S.A., Z.M. Ding, L.H. Michael, M.L. Entman, S. Daniel, and C.M. Ballantyne. 2001. Leukocyte trafficking and myocardial reperfusion injury in ICAM-1/P-selectin-knockout mice. *Am. J. Physiol. Heart Circ. Physiol.* 280:H60–H67.
8. Bowden, R.A., Z.M. Ding, E.M. Donnachie, T.K. Petersen, L.H. Michael, C.M. Ballantyne, and A.R. Burns. 2002. Role of alpha4 integrin and VCAM-1 in CD18-independent neutrophil migration across mouse cardiac endothelium. *Circ. Res.* 90:562–569.
9. Hill, J.H., and P.A. Ward. 1971. The phlogistic role of C3 leukotactic fragments in myocardial infarcts of rats. *J. Exp. Med.* 133:885–900.
10. Weisman, H.F., T. Bartow, M.K. Leppo, H.C. Marsh, G.R. Carson, M.F. Concino, M.P. Boyle, K.H. Roux, M.L. Weisfeldt, and D.T. Fearon. 1990. Soluble human complement receptor type I: in vivo inhibitor of complement suppressing post-ischemic myocardial inflammation and necrosis. *Science.* 249:146–151.
11. Chai, P.J., R. Nassar, A.E. Oakeley, D.M. Craig, G. Quick Jr., J. Jaggers, S.P. Sanders, R.M. Ungerleider, and P.A. Anderson. 2000. Soluble complement receptor-1 protects heart, lung, and cardiac myofilament function from cardiopulmonary bypass damage. *Circulation.* 101:541–546.
12. Huang, J., L. Kim, R. Mealey, H. Marsh, Y. Zhang, A. Tenner, E. Connolly, and D. Pinsky. 1999. Neuronal protection in stroke by an sLex-glycosylated complement inhibitory protein. *Science.* 285:595–599.
13. Hill, J., T.F. Lindsay, F. Ortiz, C.G. Yeh, H.B. Hechtman, and F.D. Moore. 1992. Soluble complement receptor type 1 ameliorates the local and remote organ injury after intestinal ischemia-reperfusion in the rat. *J. Immunol.* 149:1723–1730.
14. Schafer, H., D. Mathey, F. Hugo, and S. Bhakdi. 1986. Deposition of terminal C5b-9 complement complex in infarcted areas of human myocardium. *J. Immunol.* 137:1945–1949.
15. Robert-Offerman, S.R., M.P. Leers, R.J. van Suylen, M. Nap, M.J. Daemen, and P.H. Theunissen. 2000. Evaluation of the membrane attack complex of complement for the detection of a recent myocardial infarction in man. *J. Pathol.* 191:48–53.
16. Fleming, S.D., D. Mastellos, G. Karpel-Massler, T. Shea-Donohue, J.D. Lambris, and G.C. Tsokos. 2003. C5a causes limited, polymorphonuclear cell-independent, mesenteric ischemia/reperfusion-induced injury. *Clin. Immunol.* 108:263–273.
17. Homeister, J.W., P. Satoh, and B.R. Lucchesi. 1992. Effects of complement activation in the isolated heart. Role of the terminal complement components. *Circ. Res.* 71:303–319.
18. Zhao, H., M.C. Montalto, K.J. Pfeiffer, L. Hao, and G.L. Stahl. 2002. Murine model of gastrointestinal ischemia associated with complement-dependent injury. *J. Appl. Physiol.* 93:338–345.
19. Austen, W.G., Jr., C. Kyriakides, J. Favuzza, Y. Wang, L. Kobzik, F.D. Moore Jr., and H.B. Hechtman. 1999. Intestinal ischemia-reperfusion injury is mediated by the membrane attack complex. *Surgery.* 126: 343–348.
20. Kilgore, K.S., J.L. Park, E.J. Tanhehco, E.A. Booth, R.M. Marks, and B.R. Lucchesi. 1998. Attenuation of interleukin-8 expression in C6-deficient rabbits after myocardial ischemia/reperfusion. *J. Mol. Cell. Cardiol.* 30:75–85.
21. Ito, W., H.J. Schafer, S. Bhakdi, R. Klask, S. Hansen, S. Schaarschmidt, J. Schofer, F. Hugo, T. Hamdoch, and D. Mathey. 1996. Influence of the terminal complement-complex on reperfusion injury, no-reflow and arrhythmias: a comparison between C6-competent and C6-deficient rabbits. *Cardiovasc. Res.* 32:294–305.
22. Abonia, J.P., D.S. Friend, W.G. Austen Jr., F.D. Moore Jr., M.C. Carroll, R. Chan, J. Afnan, A. Humbles, C. Gerard, P. Knight, et al. 2005. Mast cell protease 5 mediates ischemia-reperfusion injury of mouse skeletal muscle. *J. Immunol.* 174:7285–7291.
23. Weiser, M., J. Williams, F. Moore, L. Kobzik, M. Ma, H. Hechtman, and M. Carroll. 1996. Reperfusion injury of ischemic skeletal muscle is

mediated by natural antibody and complement. *J. Exp. Med.* 183: 2343–2348.
24. Williams, J.P., F.D. Moore, L. Kobzik, M.C. Carroll, and H.B. Hechtman. 1999. Intestinal reperfusion injury is mediated by IgM and complement. *J. Appl. Physiol.* 86:938–942.
25. Fleming, S.D., T. Shea-Donohue, J.M. Guthridge, L. Kulik, T.J. Waldschmidt, M.G. Gipson, G.C. Tsokos, and V.M. Holers. 2002. Mice deficient in complement receptors 1 and 2 lack a tissue injury-inducing subset of the natural antibody repertoire. *J. Immunol.* 169: 2126–2133.
26. Reid, R.R., S. Woodcock, A. Shimabukuro-Vornhagen, W.G. Austen Jr., L. Kobzik, M. Zhang, H.B. Hechtman, F.D. Moore Jr., and M.C. Carroll. 2002. Functional activity of natural antibody is altered in Cr2-deficient mice. *J. Immunol.* 169:5433–5440.
27. Zhang, M., W.G. Austen Jr., I. Chiu, E.M. Alicot, R. Hung, M. Ma, N. Verna, M. Xu, H.B. Hechtman, F.D. Moore Jr., and M.C. Carroll. 2004. Identification of a specific self-reactive IgM antibody that initiates intestinal ischemia/reperfusion injury. *Proc. Natl. Acad. Sci. USA.* 101: 3886–3891.
28. Austen, W.G., Jr., M. Zhang, R. Chan, D. Friend, H.B. Hechtman, M.C. Carroll, and F.D. Moore Jr. 2004. Murine hindlimb reperfusion injury can be initiated by a self-reactive monoclonal IgM. *Surgery.* 136: 401–406.
29. Beutler, B. 2004. Inferences, questions and possibilities in Toll-like receptor signalling. *Nature.* 430:257–263.
30. Carroll, M.C., and V.M. Holers. 2005. Innate autoimmunity. *Adv. Immunol.* 86:137–157.
31. Kocks, C., R. Maehr, H.S. Overkleeft, E.W. Wang, L.K. Iyer, A.M. Lennon-Dumenil, H.L. Ploegh, and B.M. Kessler. 2003. Functional proteomics of the active cysteine protease content in drosophila S2 cells. *Mol. Cell. Proteomics.* 2:1188–1197.
32. Golomb, E., X. Ma, S.S. Jana, Y.A. Preston, S. Kawamoto, N.G. Shoham, E. Goldin, M.A. Conti, J.R. Sellers, and R.S. Adelstein. 2004. Identification and characterization of nonmuscle myosin II-C, a new member of the myosin II family. *J. Biol. Chem.* 279:2800–2808.
33. Kelley, C.A., J.R. Sellers, D.L. Gard, D. Bui, R.S. Adelstein, and I.C. Baines. 1996. Xenopus nonmuscle myosin heavy chain isoforms have different subcellular localizations and enzymatic activities. *J. Cell Biol.* 134:675–687.
34. Hart, M.L., K.A. Ceonzo, L.A. Shaffer, K. Takahashi, R.P. Rother, W.R. Reenstra, J.A. Buras, and G.L. Stahl. 2005. Gastrointestinal ischemia-reperfusion injury is lectin complement pathway dependent without involving C1q. *J. Immunol.* 174:6373–6380.
35. Hardy, R.R., C.E. Carmack, Y.S. Li, and K. Hayakawa. 1994. Distinctive developmental origins and specificities of murine CD5+ B cells. *Immunol. Rev.* 137:91–118.
36. Herzenberg, L.A., and A.B. Kantor. 1993. B cell lineages exist in the mouse. *Immunol. Today.* 14:79–83.
37. Arnold, L., C. Pennell, S. McCray, and S. Clarke. 1994. Development of B-1 cells: segregation of phosphatidyl choline–specific B cells to the B-1 population occurs after immunoglobulin gene expression. *J. Exp. Med.* 179:1585–1595.
38. Bendelac, A., M. Bonneville, and J.F. Kearney. 2001. Autoreactivity by design: innate B and T lymphocytes. *Nat. Rev. Immunol.* 1:177–186.
39. Martin, F., and J. Kearney. 2001. B1 cells: similarities and differences with other B cell subsets. *Curr. Opin. Immunol.* 13:195–201.
40. Bresnick, A.R. 1999. Molecular mechanisms of nonmuscle myosin-II regulation. *Curr. Opin. Cell Biol.* 11:26–33.
41. Zorov, D.B., C.R. Filburn, L.O. Klotz, J.L. Zweier, and S.J. Sollott. 2000. Reactive oxygen species (ROS)–induced ROS release: a new phenomenon accompanying induction of the mitochondrial permeability transition in cardiac myocytes. *J. Exp. Med.* 192:1001–1014.
42. Kolega, J. 1998. Cytoplasmic dynamics of myosin IIA and IIB: spatial "sorting" of isoforms in locomoting cells. *J. Cell Sci.* 111:2085–2095.
43. Gasser, S., S. Orsulic, E.J. Brown, and D.H. Raulet. 2005. The DNA damage pathway regulates innate immune system ligands of the NKG2D receptor. *Nature.* 436:1186–1190.
44. Fleming, S.D., R.P. Egan, C. Chai, G. Girardi, V.M. Holers, J. Salmon, M. Monestier, and G.C. Tsokos. 2004. Anti-phospholipid antibodies restore mesenteric ischemia/reperfusion-induced injury in complement receptor 2/complement receptor 1-deficient mice. *J. Immunol.* 173:7055–7061.
45. Fleming, S.D., M. Monestier, and G.C. Tsokos. 2004. Accelerated ischemia/reperfusion-induced injury in autoimmunity-prone mice. *J. Immunol.* 173:4230–4235.
46. Eisenberg, R.A., S.Y. Craven, C.L. Fisher, S.C. Morris, R. Rapoport, D.S. Pisetsky, and P.L. Cohen. 1989. The genetics of autoantibody production in MRL/lpr lupus mice. *Clin. Exp. Rheumatol.* 7:S35–S40.
47. Paimela, H., P.J. Goddard, and W. Silen. 1995. Present views on restitution of gastrointestinal epithelium. *Dig. Dis. Sci.* 40:2495–2496.
48. Fujita, T., M. Matsushita, and Y. Endo. 2004. The lectin-complement pathway—its role in innate immunity and evolution. *Immunol. Rev.* 198:185–202.
49. Vandivier, R.W., C.A. Ogden, V.A. Fadok, P.R. Hoffmann, K.K. Brown, M. Botto, M.J. Walport, J.H. Fisher, P.M. Henson, and K.E. Greene. 2002. Role of surfactant proteins A, D, and C1q in the clearance of apoptotic cells in vivo and in vitro: calreticulin and CD91 as a common collectin receptor complex. *J. Immunol.* 169:3978–3986.
50. Gardai, S.J., Y.Q. Xiao, M. Dickinson, J.A. Nick, D.R. Voelker, K.E. Greene, and P.M. Henson. 2003. By binding SIRPalpha or calreticulin/CD91, lung collectins act as dual function surveillance molecules to suppress or enhance inflammation. *Cell.* 115:13–23.
51. Taylor, P.R., A. Carugati, V.A. Fadok, H.T. Cook, M. Andrews, M.C. Carroll, J.S. Savill, P.M. Henson, M. Botto, and M.J. Walport. 2000. A hierarchical role for classical pathway complement proteins in the clearance of apoptotic cells in vivo. *J. Exp. Med.* 192:359–366.
52. Cotran, R.S., V. Kumar, and S.L. Robbins. 1994. Pathologic Basis of Disease. Fifth edition. W.B. Saunders, Philadelphia. 1425 pp.
53. Brandt, L.J. 2003. Messenteric vascular diease. *In* Current Diagnosis and Treatment in Gastroenterology. Second edition. S.L. Friedman, editor. McGraw-Hill Inc., New York. Chapter 9.
54. Chiu, C.J., A.H. McArdle, R. Brown, H.J. Scott, and F.N. Gurd. 1970. Intestinal mucosal lesion in low-flow states. I. A morphological, hemodynamic, and metabolic reappraisal. *Arch. Surg.* 101:478–483.
55. Vorup-Jensen, T., C. Ostermeier, M. Shimaoka, U. Hommel, and T.A. Springer. 2003. Structure and allosteric regulation of the alpha X beta 2 integrin I domain. *Proc. Natl. Acad. Sci. USA.* 100:1873–1878.
56. Borodovsky, A., H. Ovaa, N. Kolli, T. Gan-Erdene, K.D. Wilkinson, H.L. Ploegh, and B.M. Kessler. 2002. Chemistry-based functional proteomics reveals novel members of the deubiquitinating enzyme family. *Chem. Biol.* 9:1149–1159.
57. Wang, Q., C.H. Fang, and P.O. Hasselgren. 2001. Intestinal permeability is reduced and IL-10 levels are increased in septic IL-6 knockout mice. *Am. J. Physiol. Regul. Integr. Comp. Physiol.* 281:R1013–R1023.
58. Alencar, H., U. Mahmood, Y. Kawano, T. Hirata, and R. Weissleder. 2005. Novel multiwavelength microscopic scanner for mouse imaging. *Neoplasia.* 7:977–983.